Concept of a New Cylindrical Wind Turbine with Axial Inlet and Side Outlet Based on the Inverse Francis Principle

Ranko Artuković[1]

[1]Independent researcher, Zadar, Croatia, ORCID: 0000-0001-7434-8737, E-mail: rankoartukovic@yahoo.com

Abstract

This study presents a theoretical analysis of a cylindrical wind turbine concept featuring axial inlet and lateral outlet flow configuration. Inspired by the Francis water turbine principle operating in reverse ("inverse Francis"), we develop a mathematical model for particle-disc energy transfer and apply conservation laws to derive efficiency expressions. The analysis suggests that under idealized frictionless conditions, the inverse Francis configuration may enable high energy conversion efficiency. We propose a Wind-Eater Turbine (WET) design incorporating helically twisted blades, flow concentrator, and axial barrier. Unlike conventional horizontal-axis (HAWT) and vertical-axis (VAWT) wind turbines, the proposed closed-cylinder design operates as a semi-enclosed system where Betz's limit derivation may not directly apply. Theoretical calculations indicate potential for efficiency exceeding conventional turbine limits, though experimental validation is required. Practical challenges including fluid viscosity, turbulence, and structural constraints are discussed. The work presents a conceptual framework for further investigation through computational fluid dynamics and physical prototyping.

Keywords: inverse Francis principle, axial inlet turbine, Wind-Eater Turbine, flow concentrator, cylindrical wind turbine, helical blades, energy conversion efficiency

1 Introduction

Wind energy conversion remains a critical component of global renewable energy strategies. Conventional wind turbines are classified by rotational axis orientation: horizontal-axis wind turbines (HAWT) and vertical-axis wind turbines (VAWT). HAWTs generally achieve higher efficiency in steady wind conditions, while VAWTs offer advantages in urban environments with variable wind direction [1, 2].

A fundamental constraint on conventional open-rotor wind turbines is the Betz limit, which states that no turbine can extract more than 59.3% of kinetic energy from an open air stream under steady-state conditions [3]. This limit assumes axial flow through an open control volume with equal pressure upstream and downstream. However, in enclosed or semi-enclosed systems such as ducted turbines or reaction-type configurations, different thermodynamic constraints may apply [4].

Water turbines, particularly the Francis turbine, can achieve efficiencies exceeding 90% because they operate in enclosed systems under pressure differential conditions. The Francis turbine features radial inlet flow and axial outlet flow, with guide vanes directing water onto curved runner blades. This configuration enables efficient angular momentum transfer with minimal losses [5, 6].

This study explores a novel concept: reversing the Francis flow pattern for wind energy applications. In this "inverse Francis" configuration, flow enters axially at the turbine center and exits laterally at the periphery after traversing helically twisted channels. We hypothesize that such a semi-enclosed cylindrical design may operate under different thermodynamic constraints than open-rotor systems, potentially enabling efficiency beyond conventional limits.

Our objectives are: (1) to develop a simplified mathematical model of particle-disc energy transfer representing the inverse Francis principle; (2) to derive theoretical efficiency expressions using conservation laws; (3) to propose a practical Wind-Eater Turbine (WET) design incorporating this principle; (4) to discuss flow characteristics, design parameters, and operational considerations; (5) to identify limitations and outline requirements for experimental validation.

We emphasize that this work presents a theoretical framework and conceptual design requiring rigorous computational fluid dynamics (CFD) analysis and physical testing before practical implementation. In addition to open-rotor HAWT and VAWT concepts, various enclosed or semi-enclosed small wind turbines with axial inlet and radial or lateral outlet flow have been proposed for building-integrated applications. Such devices typically employ a disk with radially arranged blades inside a housing with a funnel-shaped inlet and lateral exhaust channels, mounted on walls or rooftops to capture façade-driven wind flows. Their operating principle relies on fan-like redirection of the incoming air and on local pressure differences generated by the housing geometry rather than on a clearly formulated reaction-turbine framework. In contrast, the present work aims to provide a theoretical inverse-Francis model that can systematically describe angular momentum transfer in a cylindrical axial-inlet / side-outlet configuration.

2 Physical Principle of the Francis Turbine

The Francis turbine converts hydraulic energy to mechanical rotation through controlled flow redirection. Water enters through a spiral casing (volute) with decreasing cross-sectional area, maintaining approximately constant angular momentum [5]. Guide vanes direct flow radially inward onto runner blades, which redirect flow to axial outlet while extracting angular momentum.

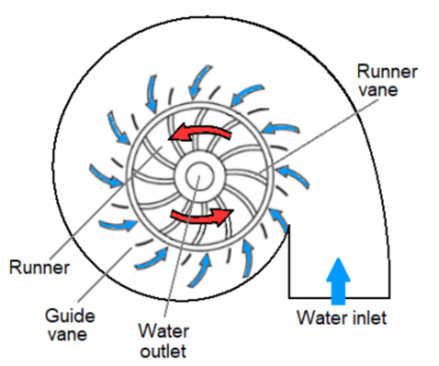

Figure 1: Schematic of Francis water turbine, top view. Water enters radially through spiral casing and exits axially.

We can illustrate the Francis principle using a simplified physical model. Consider a thin disc of radius R and moment of inertia I rotating at angular velocity ω_0 about a central axis. A semicircular duct of mean radius $\rho = R/2$ is mounted on the disc, formed by two vertical blades creating a frictionless channel from edge (point A) to center (point B).

A particle of mass m enters the duct at point A with tangential velocity v_0 and exits at center B with radial velocity v. We apply conservation of angular momentum and energy for initial state A and final state B.

Angular momentum conservation about the central axis:

$$I\omega_0 + mv_0R = I\omega + 0 \tag{1}$$

The right-hand term equals zero because radial velocity v contributes no angular momentum about the rotation axis. Final angular velocity:

$$\omega = \omega_0 + \frac{mv_0R}{I} \tag{2}$$

Energy conservation:

$$\frac{1}{2}mv_0^2 + \frac{1}{2}I\omega_0^2 = \frac{1}{2}mv^2 + \frac{1}{2}I\omega^2 \tag{3}$$

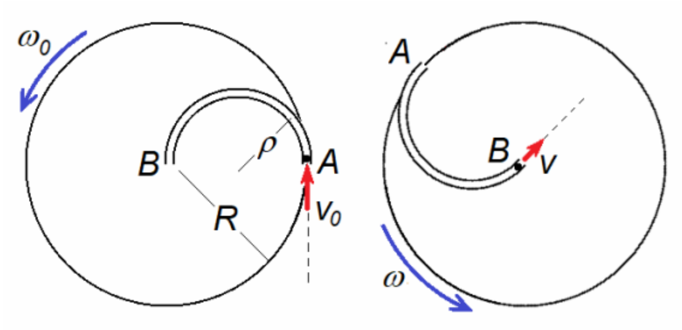

Figure 2: Simplified Francis principle model. A particle rolls along a semicircular duct from disc edge (A) to center (B). Input velocity v_0 is tangential; output velocity v is radial.

Substituting Eq. (2) into Eq. (3) and solving for v:

$$v = v_0\sqrt{1 - \frac{mR^2}{I} - \frac{2\omega_0 R}{v_0}} \tag{4}$$

For the particle to reach the disc center, initial speed must exceed:

$$v_0 > \frac{2\omega_0 R}{1 - mR^2/I} \tag{5}$$

Energy conversion efficiency from particle kinetic energy to disc rotational energy:

$$\eta = \frac{\Delta K}{K_0} = \frac{K_0 - K}{K_0} = 1 - \left(\frac{v}{v_0}\right)^2 \tag{6}$$

As v_0 approaches the threshold value Eq. (5), output velocity $v \to 0$ and efficiency $\eta \to 1$ (100%). This idealized frictionless model demonstrates efficient kinetic energy transfer from particle to disc rotation.

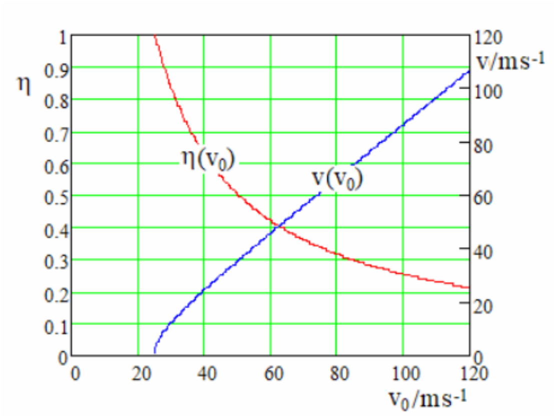

Figure 3: Francis principle: output velocity $v(v_0)$ and efficiency $\eta(v_0)$ for example parameters $R = 0.25$ m, $I = 3$ kg m^2, $\omega_0 = 50$ s^{-1}, $m = 0.1$ kg.

3 Inverse Francis Principle

We now consider the reverse flow direction: particle enters at disc center with radial velocity v_0 and exits at periphery with tangential velocity v. This "inverse Francis" configuration is the theoretical foundation for our proposed wind turbine.

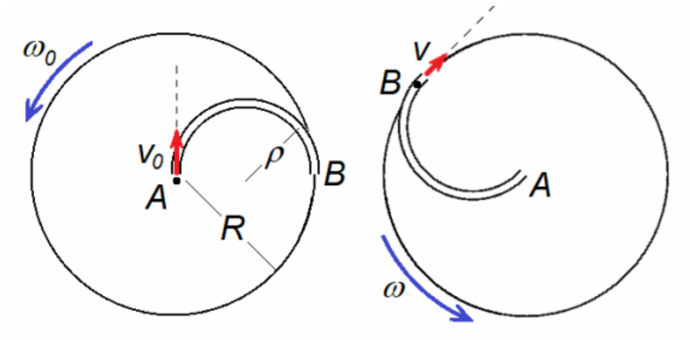

Figure 4: Inverse Francis principle. Particle enters at center with radial velocity v_0 and exits at periphery with tangential velocity v.

Angular momentum conservation:

$$I\omega_0 + 0 = I\omega - mvR \tag{7}$$

The negative sign indicates that particle exits with angular momentum opposite to disc rotation. Final angular velocity:

$$\omega = \omega_0 + \frac{mvR}{I} \tag{8}$$

Energy conservation:

$$\frac{1}{2}mv_0^2 + \frac{1}{2}I\omega_0^2 = \frac{1}{2}mv^2 + \frac{1}{2}I\omega^2 \tag{9}$$

Substituting Eq. (8) into Eq. (9) yields a quadratic equation:

$$av^2 + bv + c = 0 \tag{10}$$

where

$$a = 1 + \frac{mR^2}{I}, \quad b = 2R\omega_0, \quad c = -v_0^2 \tag{11}$$

The positive solution is:

$$v = \frac{-\omega_0 R + \sqrt{\omega_0^2 R^2 + av_0^2}}{a} \tag{12}$$

Efficiency (Eq. (6)) now depends on both ω_0 and v_0.

Example: For $R = 1$ m, $I = 3$ kg m^2, $\omega_0 = 50$ s^{-1}, $m = 0.1$ kg, $v_0 = 20$ m s^{-1}, we obtain $v = 3.85$ m s^{-1}, $\omega = 50.128$ s^{-1}, and $\eta = 96.3\%$.

As shown in Fig. 5, efficiency increases with disc angular velocity ω_0. For continuous particle flow, each successive particle incrementally increases disc rotation:

$$\omega_n = \omega_{n-1} + \frac{mR}{aI}\left(\sqrt{\omega_{n-1}^2 R^2 + av_0^2} - \omega_{n-1}R\right) \tag{13}$$

This positive feedback mechanism causes the disc to accelerate with increasing efficiency as rotation rate grows.

Theoretical claim: Under idealized frictionless conditions, the inverse Francis configuration enables energy conversion efficiency approaching 100% as disc rotation rate increases, potentially exceeding the Betz limit applicable to open-flow turbines.

Critical caveat: This claim requires experimental validation. The idealized particle model neglects viscous losses, turbulence, blade drag, and structural constraints present in real fluid flow.

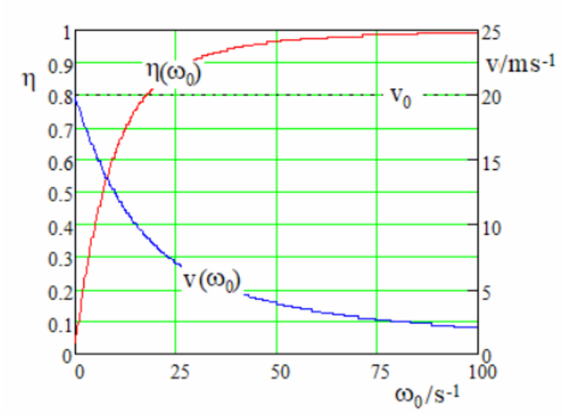

Figure 5: Inverse Francis principle: output velocity $v(\omega_0)$ and efficiency $\eta(\omega_0)$ for constant $v_0 = 20$ m s^{-1} and varying disc rotation rate.

4 From Physical Model to Turbine Design

4.1 Cylindrical blade geometry

To implement the inverse Francis principle in a wind turbine, we design helically twisted blades within a cylindrical envelope of radius R (Fig. 6). Each blade forms a spatial surface created by helical twisting of a half-cylinder of radius $R/2$ around the central axis.

Figure 6: Helically twisted blade geometry shown from four viewing angles. Three blades with open design (wide inter-blade spacing).

The helix pitch p (axial distance per complete rotation) relates to helix angle α by:

$$p = \frac{2\pi R}{\tan\alpha} \tag{14}$$

Twist angle θ over turbine length L:

$$\theta = 360\frac{L}{p} \tag{15}$$

Aspect ratio:

$$A_r = \frac{L}{2R} \tag{16}$$

Example: For $R = 1$ m, $L = 1.57$ m ($A_r = 0.785$), $\theta = 90$, we obtain $p = 6.28$ m and $\alpha = 45$.

4.2 Open versus closed blade design

We distinguish two configurations (Fig. 7):

Open-blade type: Wide spacing between adjacent blades allows free lateral flow with minimal flow restriction.

Closed-blade type: Narrow inter-blade channels act as nozzles. Each blade ABC consists of inner segment AB (radius $R/2$) and tangential extension BC (radius R). This creates confined spiral channels directing flow tangentially outward.

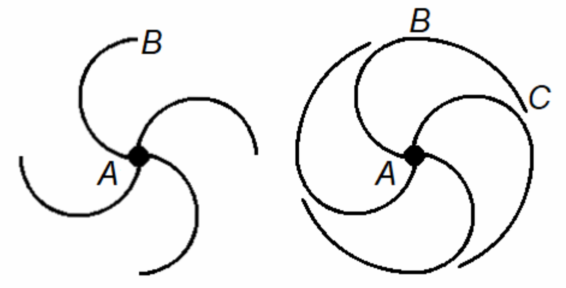

Figure 7: Cross-sectional view of 4-blade turbine. Left: open-blade type with wide inter-blade gaps. Right: closed-blade type with narrow tangential nozzles.

The closed-blade design more closely approximates the idealized model (Fig. 4) by constraining flow along semicircular paths.

5 Wind-Eater Turbine (WET) Design

5.1 System components

The complete WET assembly (Figs. 8 and 9) comprises:

1. **Front plate** with central circular aperture of diameter $d_1 < D$ (where $D = 2R$)
2. **Conical flow concentrator** directing ambient wind toward central inlet
3. **Axial barrier** (rear plate) preventing axial flow exit
4. **Central shaft** serving as rotation axis
5. **Helical blades** creating spiral channels
6. **Lateral outlet channels** between adjacent blade edges

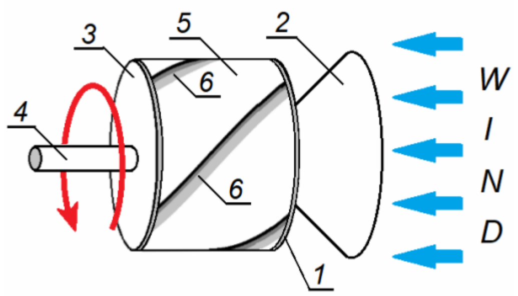

Figure 8: WET rotor with closed-blade design, perspective view. Rotation direction indicated. Components: (1) front plate, (2) flow concentrator, (3) axial barrier, (4) central shaft, (5) helical blades, (6) lateral outlet channels.

Wind enters axially through the concentrator, flows along helical blade channels while transferring angular momentum, and exits laterally through peripheral nozzles. The axial barrier prevents direct axial throughflow, forcing lateral exit.

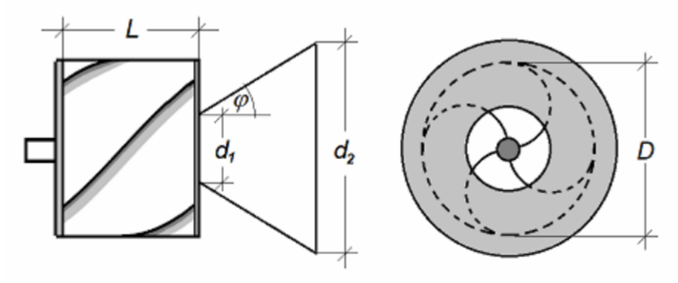

Figure 9: WET schematic views. Left: side view showing concentrator inlet diameter d_1, outlet diameter d_2, and turbine length L. Right: front view showing turbine diameter D.

5.2 Flow concentrator function

The conical concentrator serves multiple purposes:

- **Flow acceleration:** Converging geometry accelerates incoming wind according to mass continuity
- **Capture area increase:** Effective wind-capture area exceeds turbine frontal area
- **Pressure gradient:** Creates favorable pressure distribution at turbine inlet

Beyond these basic functions, in practical enclosed turbines, the inlet cone and the immediate edge geometry play a crucial role in shaping the pressure field and controlling flow separation near the front plate. Designs used in wall-mounted axial-inlet / radial-outlet turbines often employ a funnel-shaped shroud with a separation edge that splits the incoming stream into an inner branch directed toward the rotor and an outer branch guided around the housing, thereby creating a local suction region downstream of the edge. Inspired by such solutions, the WET concentrator and front-plate edges can be shaped to promote a stable attachment of the incoming flow on the inner surface while encouraging clean detachment of the outer stream, reducing recirculation and enhancing the effective pumping effect of the rotor.

For incompressible flow through the concentrator:

$$v_1 A_1 = v_2 A_2 \quad \Rightarrow \quad v_2 = v_1 \frac{d_2^2}{d_1^2} \tag{17}$$

where v_1 is ambient wind speed, v_2 is inlet velocity, and $d_2 > d_1$.

5.3 Pumping effect and self-acceleration

As turbine rotation accelerates (following Eq. (13)), centrifugal forces create radial pressure gradients within the blade channels. This induces a low-pressure region near the central inlet, potentially enhancing mass flow rate beyond ambient wind pressure alone — a pumping effect analogous to centrifugal fans.

Combined with increasing efficiency at higher rotation rates (Fig. 5), this suggests a positive feedback mechanism: initial wind input accelerates the turbine, increasing efficiency and pumping effect, further accelerating rotation. However, this idealized behavior will be limited by:

- Viscous drag on blades and internal surfaces
- Turbulent losses in blade channels
- Outlet flow resistance
- Structural vibration and bearing friction

Characteristic	HAWT / VAWT	WET (proposed)
Flow configuration	Axial inlet/outlet	Axial inlet / lateral outlet
System type	Open	Semi-enclosed
Betz limit applicability	Directly applicable	Questionable
Dominant mechanism	Lift/drag forces	Angular momentum transfer
Rotation initiation	Immediate	Requires startup acceleration
Theoretical max efficiency	59.3%	Potentially higher (unverified)

Table 1: Comparison between conventional turbines and proposed WET design.

5.4 Comparison with conventional turbines

Table 1 summarizes key differences between WET and conventional designs.

6 Limitations and Assumptions

The theoretical analysis presented relies on several idealizations:

Frictionless flow: Real air flow experiences viscous drag along blade surfaces, reducing efficiency. Boundary layer separation may occur at high angles of attack.

Inviscid particle model: Actual air is a compressible viscous fluid, not discrete particles. Turbulence, vortex shedding, and flow separation are neglected.

Steady-state assumption: The model assumes quasi-steady flow. Transient effects during startup and variable wind conditions are not addressed.

Structural constraints: Blade deformation under aerodynamic loads, bearing friction, and generator back-torque are not included.

Betz limit inapplicability: The claim that Betz's limit does not apply rests on the semi-enclosed system argument. However, energy extraction ultimately depends on kinetic energy removal from the wind, which may still impose thermodynamic limits.

Reynolds number effects: Turbine performance will depend strongly on Reynolds number, which governs boundary layer behavior and flow regime transitions.

Experimental validation required: All efficiency claims are theoretical predictions requiring rigorous CFD simulation and physical prototype testing.

7 Design Parameters and Operational Considerations

7.1 Blade number and solidity

Blade solidity (ratio of blade area to swept area) affects flow blockage and torque generation. Low solidity (2-3 blades) reduces drag but may allow flow bypass. High solidity (6-8 blades) increases torque but also drag. Optimal solidity requires CFD optimization.

7.2 Helix angle selection

Helix angle α determines flow path curvature. Small angles ($\alpha < 30$) create long, gradual paths with lower pressure drop but require greater turbine length. Large angles ($\alpha > 60$) create abrupt flow redirection with potential separation. Optimal range likely $30 < \alpha < 50$.

7.3 Concentrator geometry

Concentrator expansion ratio d_2/d_1 trades inlet velocity (Eq. (17)) against flow separation risk. Excessive expansion causes boundary layer separation and vortex formation. Cone half-angle typically 7-10° to avoid separation [4, 7].

7.4 Material selection

For prototype development, lightweight high-strength materials are essential:

- **Blades:** Carbon fiber composites, fiberglass, or ABS thermoplastic (3D printing)
- **Structural components:** Aluminum alloys for weight reduction
- **Bearings:** Low-friction sealed ball bearings

7.5 Generator coupling

During startup, the generator must operate in idle mode (minimal back-torque) to allow turbine acceleration. Once rotational speed and efficiency increase, the generator switches to power extraction mode. Variable-resistance load or power electronics enable optimal matching.

7.6 Rotor construction and balancing

For practical implementation, the WET rotor can benefit from a segmented ring construction rather than a monolithic cylindrical shell. Similar to disk-type enclosed turbines that employ a spoked wheel with circular segments to reduce mass and simplify manufacturing, the WET blades may be assembled from modular helical segments mounted on a lightweight ring frame attached to the central shaft. Such a configuration facilitates dynamic balancing by allowing the addition of small counterweights on the ring or hub and enables easy replacement or variation of blade segments for experimental studies.

Furthermore, experience from enclosed axial-inlet / radial-outlet devices suggests that adding a peripheral mass ring to the rotor can act as a flywheel, smoothing short-term wind fluctuations and reducing sensitivity to gust-induced transients. In the WET concept, a detachable mass ring integrated with the outer blade tips or ring frame could be used during prototype testing to study the trade-off between start-up behavior, rotational smoothness, and structural loads.

8 Future Research Directions

8.1 Computational fluid dynamics

High-fidelity CFD simulation (using OpenFOAM, ANSYS Fluent, or COMSOL) is essential to:

- Validate flow patterns within helical channels
- Quantify viscous losses and turbulence effects
- Optimize blade geometry, helix angle, and solidity
- Calculate realistic efficiency under varying wind speeds
- Assess pressure distribution and structural loads

Reynolds-Averaged Navier-Stokes (RANS) with k-ε or k-ω turbulence models provide reasonable initial estimates. Large Eddy Simulation (LES) offers higher accuracy but at greater computational cost.

8.2 Experimental validation

Physical prototype testing in a controlled wind tunnel environment is critical:

- Small-scale prototype ($D = 0.3$-0.5 m) fabricated via 3D printing
- Wind tunnel testing at varying speeds ($v_1 = 5$-15 m/s)
- Measurement of torque, rotational speed, power output
- Flow visualization (smoke, PIV) to observe streamline patterns
- Efficiency calculation: $\eta = P_{out}/P_{available}$

8.3 Performance optimization

Parametric studies should explore:

- Blade count: 2, 3, 4, 6, 8 blades
- Helix angle: 20, 30, 45, 60
- Aspect ratio: $A_r = 0.5, 1.0, 1.5, 2.0$
- Concentrator ratio: $d_2/d_1 = 1.5, 2.0, 2.5$
- Blade thickness and profile shape

In addition to purely aerodynamic optimization, future studies should consider structural variants inspired by existing enclosed axial-inlet / radial-outlet turbines, such as segmented rotors with peripheral mass rings and tailored shroud edges. Parametric CFD and experimental campaigns could treat rotor segmentation, edge curvature of the inlet cone, and the geometry of lateral exhaust openings as design variables, assessing their combined impact on pumping strength, noise generation, and overall efficiency.

8.4 Scaling considerations

If prototype testing validates the concept, scaling to practical sizes (e.g., D = 2-5 m) introduces additional challenges:

- Structural integrity under wind loads
- Manufacturing precision for blade geometry
- Dynamic balancing to minimize vibration
- Economic viability versus conventional turbines

9 Conclusion

This study presents a theoretical framework for a cylindrical wind turbine based on the inverse Francis principle, featuring axial inlet and lateral outlet flow configuration. Mathematical analysis using conservation laws suggests that under idealized frictionless conditions, such a configuration may enable energy conversion efficiency exceeding the Betz limit applicable to open-flow turbines.

The proposed Wind-Eater Turbine (WET) incorporates helically twisted blades, conical flow concentrator, and axial barrier to implement this principle. Theoretical predictions indicate potential for high efficiency through angular momentum transfer and centrifugal pumping effects.

However, we emphasize that these results are based on simplified models neglecting viscous losses, turbulence, and structural constraints. The primary contributions of this work are:

1. Derivation of energy transfer efficiency for idealized inverse Francis particle-disc interaction
2. Conceptual design of a cylindrical turbine implementing this principle
3. Identification of key design parameters and operational considerations
4. Clear articulation of limitations and required validation steps

Experimental validation through computational fluid dynamics and physical prototype testing is essential before practical implementation. If validated, the WET concept may offer a complementary approach to conventional HAWT and VAWT designs, particularly for low-speed or turbulent wind environments.

We encourage researchers in wind energy and fluid mechanics to investigate this concept through rigorous simulation and experimentation. All theoretical predictions presented should be viewed as hypotheses requiring empirical verification.

The existence of small enclosed axial-inlet / radial-outlet wind devices, particularly those designed for wall or rooftop mounting, indicates that semi-enclosed, disk-type configurations are already considered attractive for distributed generation, even though their operation has not yet been systematically analyzed within an inverse Francis framework.

Acknowledgments

This work is dedicated to my granddaughter Magdalena, whose cheerful presence accompanied its writing.

References

[1] Johari MK, Jalil MAA, Shariff MFM (2018) Comparison of horizontal axis wind turbine (HAWT) and vertical axis wind turbine (VAWT). *Int J Eng Technol* 7:74–80

[2] Óskarsdóttir MÓ (2014) A general description and comparison of horizontal axis wind turbines and vertical axis wind turbines. Master's thesis, University of Iceland

[3] Ragheb M, Ragheb AM (2011) Wind turbines theory — the Betz equation and optimal rotor tip speed ratio. In: Carriveau R (ed) Fundamental and advanced topics in wind power. InTech. https://doi.org/10.5772/21398

[4] Shikha, Bhatti TS, Kothari DP (2003) A new vertical axis wind rotor using convergent nozzles. In: Proc Large Engineering Conf Power Engineering, Montreal, pp 177–181

[5] Date A, Akbarzadeh A (2010) Design and analysis of a split reaction water turbine. *Renew Energy* 35:1947–1955

[6] Farriza MB, Boejanga H, Masjurib M, Arasc MSM, Razikd NHA, Mate S, Sopiane K (2015) Evolution of simple reaction type turbines for pico-hydro applications. *Jurnal Teknologi* 77:1–9

[7] Shonhiwa C, Makaka G (2016) Concentrator augmented wind turbines: a review. *Renew Sustain Energy Rev* 59:1415–1418

[8] Chen CC, Kuo CH, Hsieh WC, Miao JM (2011) What happens to the Betz limit in VAWT system? In: Proc 13th Int Conf Wind Engineering, Amsterdam

[9] Saha UK, Rajkumar MJ (2006) On the performance analysis of Savonius rotor with twisted blades. *Renew Energy* 31:1776–1788

[10] Lajnef M, Mosbahi M, Chouaibi Y, Driss Z (2020) Performance improvement in a helical Savonius wind rotor. *Arab J Sci Eng* 45:9305–9323

[11] Lee JH, Lee YT, Lim HC (2016) Effect of twist angle on the performance of Savonius wind turbine. *Renew Energy* 89:231–244

[12] Date A, Date A, Akbarzadeh A (2012) Performance investigation of a simple reaction water turbine for power generation from low head micro hydro resources. *Smart Grid Renew Energy* 3:239–245

[13] Ding L, Guo T (2020) Numerical study on the power efficiency and flow characteristics of a new type of wind energy collection device. *Appl Sci* 10:7438

[14] Artuković R (2014) Planar motion of a pointlike mass along a rotating guideline. *Eur J Phys* 35:065014